

Magnetic field effects in the Anderson model of dilute magnetic alloys. II. Numerical results

Gee Swee Poo*

Physics Department, University of Malaya, Kuala Lumpur, Malaysia
and Department of Mathematics, Imperial College, London, S.W.7, United Kingdom

(Received 10 June 1974)

A numerical study is made on the magnetic field effects of the infinite- U Anderson Hamiltonian, using the analytic solution derived in a preceding paper. The impurity magnetization, the magnetoresistivity, and the Hall coefficient are calculated. The resulting family of curves of the magnetoresistivity exhibits consistent plateau regions at low temperatures. This is in good qualitative agreement with the experiments of Fenton on Fe and Cr in a Cu(Au) matrix and with those of Daybell and Steyert on Cr in Cu. An approximate but analytic expression for the magnetoresistivity is also derived. The Hall coefficient is found to increase with field and has a zero slope for vanishingly small fields. This is in agreement with calculations based on the s - d exchange model. For temperatures above the Kondo temperature, we find that the Hall coefficient and the negative magnetoresistivity are proportional to each other and to the square of the impurity magnetization.

I. INTRODUCTION

In the preceding paper,¹ hereafter referred to as I, we treated the field-dependent infinite- U Anderson Hamiltonian in a self-consistent manner by means of the double-time Green's-function method. The resulting solutions can be summarized as follows:

$$G_{kk}^{\sigma}(\omega) = \frac{1}{2\pi} \left(\frac{1}{\omega - \epsilon_{k\sigma}} + \frac{V^2 t^{\sigma}(\omega)}{(\omega - \epsilon_{k\sigma})^2} \right), \quad (1.1)$$

$$t^{\sigma}(\omega - \sigma H \pm i\delta) = \mp \frac{i}{2\Delta} [1 - \psi^{\sigma}(\omega - \sigma H \pm i\delta)], \quad (1.2)$$

$$\begin{aligned} \psi^{\dagger}(\omega - H + i\delta) &= \frac{W_0(\omega)[B_1(\omega) - iA_1(\omega)]}{[H_1^D(\omega)]^{1/2}} \\ &\quad \times \left(\frac{H_1^{-1}(\omega)}{H_2(\omega)} \right)^{1/4} e^{Q_3(\omega)}, \end{aligned} \quad (1.3)$$

$$\begin{aligned} \psi^{\dagger}(\omega + H - i\delta) &= \frac{B_2(\omega) + iA_2(\omega)}{W_0(\omega)[H_1^D(\omega)]^{1/2}} \\ &\quad \times \left(\frac{H_1^{-1}(\omega)}{H_2(\omega)} \right)^{-1/4} e^{-Q_3(\omega)}, \end{aligned} \quad (1.4)$$

$$Q_3(\omega) = \frac{i}{4\pi} P \int_{-D}^D d\xi \frac{\ln[H_1^{-1}H_2(\xi)]}{\omega - \xi}, \quad (1.5)$$

$$W_0(\omega) = \left(\frac{1 + ie(\omega) + N_0/3\pi}{1 - ie(\omega) - M_0/3\pi} \right)^{1/2}, \quad (1.6)$$

$$M_r = -\Delta^{-r-1} \int_{-D}^D \omega^r \ln[H_1^{-1}(\omega)] d\omega, \quad (1.7)$$

$$N_r = \Delta^{-r-1} \int_{-D}^D \omega^r \ln[H_2(\omega)] d\omega, \quad (1.8)$$

$$H_1^{-1}(\omega) = [U_1(\omega) + iV_1(\omega)]/H_1^D(\omega), \quad (1.9)$$

$$H_2(\omega) = [U_2(\omega) + iV_2(\omega)]/H_1^D(\omega), \quad (1.10)$$

$$H_1^D(\omega) = J_1(\omega) + iL_1(\omega), \quad (1.11)$$

$$\begin{aligned} U_{1,2}(\omega) &= 1 + \text{Re}C - d^{\dagger}d^{\dagger} + B_{2,1}(\omega)B_{3,4}(\omega) \\ &\quad + A_1(\omega)A_2(\omega), \end{aligned} \quad (1.12)$$

$$\begin{aligned} V_{1,2}(\omega) &= \text{Im}C + e(\omega)(d^{\dagger} - d^{\dagger}) + A_2(\omega)B_{3,1}(\omega) \\ &\quad - A_1(\omega)B_{2,4}(\omega), \end{aligned} \quad (1.13)$$

$$J_1(\omega) = 1 + \text{Re}C - d^{\dagger}d^{\dagger} + B_1(\omega)B_2(\omega) + A_1(\omega)A_2(\omega), \quad (1.14)$$

$$\begin{aligned} L_1(\omega) &= \text{Im}C + e(\omega)(d^{\dagger} - d^{\dagger}) + B_1(\omega)A_2(\omega) \\ &\quad - A_1(\omega)B_2(\omega), \end{aligned} \quad (1.15)$$

$$B_{1,3}(\omega) = d^{\dagger} \pm F_1(\omega), \quad B_{2,4}(\omega) = d^{\dagger} \mp F_2(\omega), \quad (1.16)$$

$$A_{1,2}(\omega) = \frac{2}{3\pi} \left[\frac{\pi\omega}{\Delta} + \ln \left(\frac{T}{T_K} \frac{D}{(D^2 - \omega^2)^{1/2}} \right) + \phi \left(\frac{\omega \pm H}{2\pi T} \right) \right], \quad (1.17)$$

$$\phi(y) = \text{Re}[\Psi(\frac{1}{2} \mp iy) - \Psi(\frac{1}{2})], \quad (1.18)$$

$$F_{1,2}(\omega) = \mp \frac{1}{3} \tanh \left(\frac{\omega \pm H}{2T} \right), \quad (1.19)$$

$$H_K/D = \pi T_K/2\alpha D = e^{\pi\epsilon_d/\Delta}, \quad (1.20)$$

$$\text{Re}C = \frac{4}{3} (\langle n_{\uparrow} \rangle + \langle n_{\downarrow} \rangle - \frac{2}{3}), \quad (1.21)$$

$$e(\omega) = 2(\omega - \epsilon_d)/3\Delta, \quad (1.22)$$

$$d^{\sigma} = \frac{1}{3}(4 \langle n_{\sigma} \rangle - 1). \quad (1.23)$$

The above solutions are valid for the situation of interest, $\omega, T, H \ll D$. They contain three unknowns $\langle n_{\uparrow} \rangle$, $\langle n_{\downarrow} \rangle$, and $\text{Im}C$ which are to be determined self-consistently from the three independent transcendental equations [(I3.35), (I3.39), and (I3.40)] obtained in I. Straightforward computation is complicated in view of the fact that there are as many as five parameters to vary. To simplify the matter, we introduce an auxiliary condition. We make use of the fact that the total impurity-electron oc-

cupation number at the impurity levels is always conserved before and after the application of an external magnetic field. This gives

$$\langle n_+ \rangle + \langle n_- \rangle = 2 \langle n \rangle, \quad (1.24)$$

where $\langle n \rangle$ is the zero-field occupation number which has been investigated in detail in I. With the auxiliary condition, we are able to reduce the three transcendental equations to two, thus, greatly simplifying the numerical procedure.

In this paper, we present the results of an exact numerical calculation of the occupation numbers $\langle n_+ \rangle$ and $\langle n_- \rangle$, the impurity magnetization, the magnetoresistivity, and the Hall coefficient. The results are analyzed and compared with experiments and other theoretical calculations.

II. NUMERICAL COMPUTATION AND IMPURITY MAGNETIZATION

The variables $\langle n_+ \rangle$, $\langle n_- \rangle$ and, $\text{Im}C$ are to be determined from the following equations

$$\langle n_+ \rangle = \frac{1}{2}(1 - \langle n_- \rangle) + \frac{H}{2\pi\Delta} - \frac{\text{Im}N_1}{4\pi} + \frac{3\text{Re}N_0}{8\pi} + \frac{\epsilon_d \text{Im}N_0}{4\pi\Delta} + \frac{1}{16\pi^2} [(\text{Re}N_0)^2 - (\text{Im}N_0)^2], \quad (2.1)$$

$$\begin{aligned} \text{Im}C = & \frac{2}{9\pi} (\text{Re}M_1 + \text{Re}N_1) - \frac{1}{3\pi} (\text{Im}M_0 - \text{Im}N_0) \\ & - \frac{2\epsilon_d}{9\pi\Delta} (\text{Re}M_0 + \text{Re}N_0) + \frac{1}{9\pi^2} (\text{Re}M_0 \text{Im}M_0 \\ & + \text{Re}N_0 \text{Im}N_0), \end{aligned} \quad (2.2)$$

with $\langle n_+ \rangle$ given in (1.24). These integral equations are solved numerically using the standard Newton's method for simultaneous nonlinear equations.²

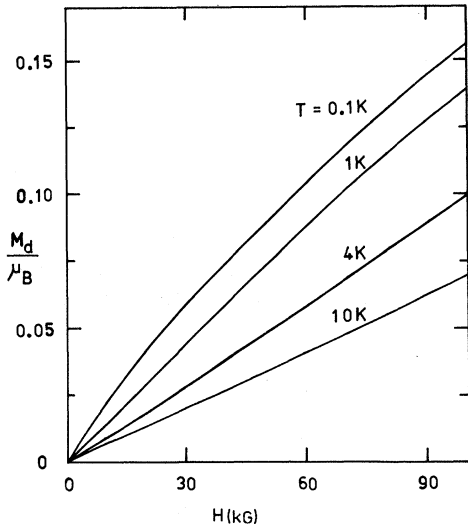


FIG. 1. Impurity magnetization M_d as a function of the external magnetic field for a number of temperatures.

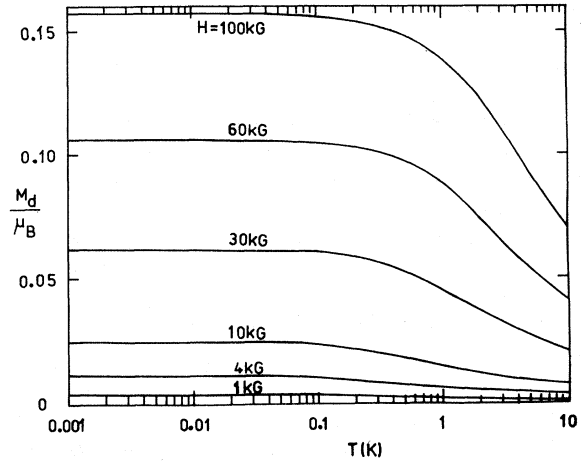


FIG. 2. Impurity magnetization M_d as a function of temperature for a number of external magnetic fields.

The iteration procedure involved converges easily provided the Jacobian of the above functions does not vanish and the initial approximation is chosen sufficiently close to the actual root. The moments M_r and N_r , and their partial derivatives, are evaluated by the usual Romberg integration techniques.² The interval $(-D, D)$ is subdivided into many subintervals such that each can be computed to the desired accuracy. Absolute accuracy of 10^{-4} is ensured for the final values of $\langle n_+ \rangle$, $\langle n_- \rangle$, and $\text{Im}C$.

For simplicity, we have chosen the parameters $D = 2 \times 10^4$ K, $\epsilon_d = -0.05D$, and $T_K = 2$ K throughout the entire computation. Then Δ is determined by ϵ_d and T_K via the equation for T_K , (1.20). For each set of values of H and T , we solve equations (2.1), (2.2), and (1.24) for the variables $\langle n_+ \rangle$, $\langle n_- \rangle$, and $\text{Im}C$ using the appropriate value of $\langle n \rangle$ which has been evaluated in I. The functions $\text{Re}M_0$, $\text{Im}M_0$, $\text{Re}N_0$, and $\text{Im}N_0$ are then calculated. The solution together with the properly evaluated functions are to be used in the subsequent computation of the magnetoresistivity and the Hall coefficient.

The impurity magnetization M_d is given by

$$M_d = \mu_B (\langle n_+ \rangle - \langle n_- \rangle). \quad (2.3)$$

We note that M_d represents only the local magnetization due to the impurity spin and not the bulk magnetization. The field and temperature dependence of M_d are shown in Figs. 1 and 2. For temperatures above T_K , the d magnetization is roughly a monotonic increasing function of H . For $T < T_K$, a certain amount of curvature appears but it is not large enough to indicate any sign of approaching saturation. Strong temperature dependence of M_d is only observed at high temperatures and high fields as indicated in Fig. 2. For temperatures

much below T_K , the curves are practically independent of T .

The results show general agreement with the theoretical calculations of Nam and Woo³ and of Bloomfield, Hecht, and Sievert,⁴ although our low-temperature curves do not vary as rapidly as theirs (see Fig. 4 of Ref. 4). Experimentally, the bulk magnetization of the isolated Fe impurity in Cu-Fe alloys has been determined by Tholence and Tournier⁵ and by Franz and Sellmyer.⁶ Their results give general features similar to those shown in Fig. 1. However, as we are not certain about the conduction-electron contribution to the magnetization in our system, the comparison cannot be serious.

The quantity $-\text{Im}C$ is found to vary with M_d linearly as shown in Fig. 3. For all temperatures (from 0.001 to 10 K) computed, a single straight line is obtained. This leads to the conjecture that $-\text{Im}C = b_m M_d$ where the slope b_m is independent of temperature but depends sensitively on the choice of ϵ_d . For $\epsilon_d = -0.05D$, b_m is close to unity. The functions M_r and N_r exhibit similar weak dependence on fields and temperatures. The field variations of $\text{Re}M_0$ and $\text{Im}M_0$ are shown in Figs. 4 and 5 for the purpose of illustration. Figure 4 shows a monotonic increase of $\text{Re}M_0$ with H . In Fig. 5, the low-temperature curves of $-\text{Im}M_0$ show an initial dip, whereas the high-temperature curves increase steadily with fields. For fields up to 80 kG, $\text{Re}M_0$ shows a change of about 15%. Compared with the unity factor, its influence is felt only at high fields and low temperatures. As for $-\text{Im}M_0$,

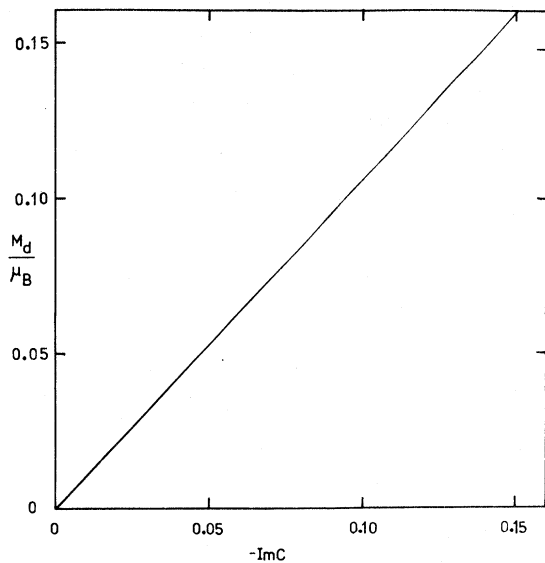


FIG. 3. Impurity magnetization M_d/μ_B versus $-\text{Im}C$ for fields up to 100 kG and temperatures ranging from 0.001 to 10 K.

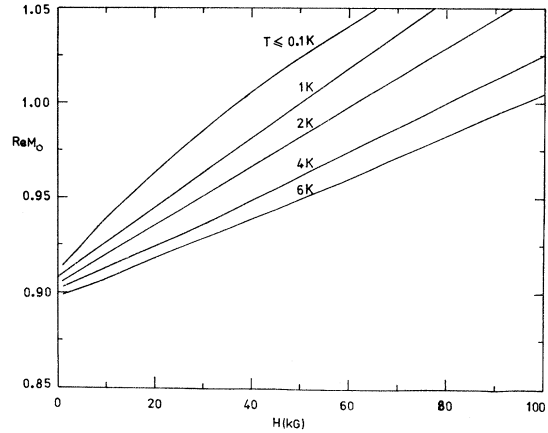


FIG. 4. $\text{Re}M_0$ as a function of the external magnetic field for a number of temperatures.

the change is very small, less than 0.1%. Hence, it can be discarded in the presence of $e(0)$.

III. MAGNETORESISTIVITY

The longitudinal magnetoresistivity is the reciprocal of the static conductivity σ_L , given by

$$\sigma_L = -\frac{e^2}{3} \int d\omega \rho(\omega) v^2(\omega) \sum_{\sigma} \tau_{\sigma}(\omega) \frac{\partial f^{\sigma}}{\partial \omega}, \quad (3.1)$$

where $\rho(\omega)$ is the density of states of the host metal, $v(\omega)$ is the electronic velocity, $\tau_{\sigma}(\omega)$ is the relaxation time for an electron of spin σ , and $f^{\sigma} \equiv f(\omega + \sigma H)$ is the Fermi distribution function. Each spin distribution has its own relaxation time

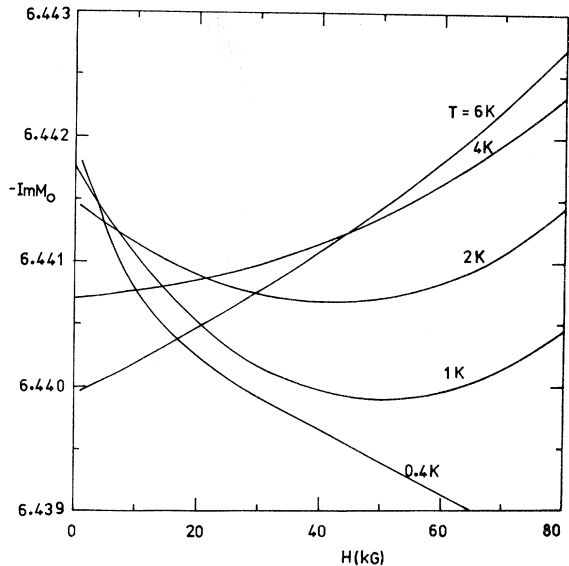


FIG. 5. $-\text{Im}M_0$ as a function of the external magnetic field for a number of temperatures.

and equilibrium distribution. The relaxation time is given by the imaginary part of the scattering amplitude

$$\tau_{\sigma}^{-1}(\omega) = \mp \frac{2\Delta C_i}{\pi\rho_0} \text{Im}t^{\sigma}(\omega \pm i\delta), \quad (3.2)$$

where C_i denotes the impurity concentration and t^{σ} is related to ψ^{σ} by (1.2). The square of the electronic velocity is given by

$$v^2(\omega) = v_F^2(1 + \bar{a}\omega/D)$$

where v_F is the Fermi velocity and \bar{a} is a constant of order less than unity. For transport properties at low T_K , $\omega \ll D$, we can approximate $v^2(\omega) \approx v_F^2$. The density of states $\rho(\omega)$ is given by ρ_0 for a square band. With these simplifications, we can express the magnetoresistivity as

$$\rho_L/\rho_L^0 = 1/P_0, \quad (3.3)$$

where

$$P_0 = \int d\omega \left(\frac{-\partial f'/\partial\omega}{1 - \text{Re}\psi'(\omega + i\delta)} + \frac{-\partial f'/\partial\omega}{1 - \text{Re}\psi'(\omega - i\delta)} \right) \quad (3.4)$$

and

$$\rho_L^0 = 2m^*C_i/Ne^2\pi\rho_0. \quad (3.5)$$

Note that we have preserved the energy averaging effect in (3.4).

At low temperatures the derivatives of the Fermi functions are sharply peaked at $\omega = \mp H$, so it is a common practice to approximate the integrals (3.1) at the values $\omega = \mp H$. The resistivity then gives

$$\rho_L^{-1} = \sigma_L = (Ne^2/2m^*)[\tau,(-H) + \tau, (H)]. \quad (3.6)$$

This formula has been widely adopted in many calculations.^{4,7,8}

It is obvious that the energy average of τ is ig-

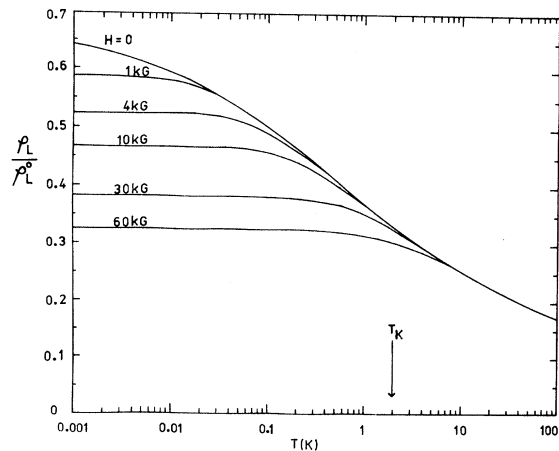


FIG. 6. Magnetoresistivity ρ_L , in reduced units, as a function of temperature for $T_K = 2$ K and a number of external magnetic fields.

nored in (3.6). We note that this approximation is not too good since at low temperatures $\text{Im}t(\omega)$ is a rapidly varying function of ω . In fact, it has been shown by Suhl⁹ that such an approximation will lead to a 20% effect in the temperature dependence of the zero-field resistivity.

Using the general expressions (3.3), (3.4), and (1.1)–(1.23), we have calculated the magnetoresistivity by means of numerical computation. For this purpose, (1.5) is rewritten as

$$Q_3(\omega) = \frac{-i}{4\pi} \left(P \int_{-D}^D \frac{g_1(\xi) - g_1(\omega)}{\xi - \omega} + g_1(\omega) \ln \left| \frac{D - \omega}{D + \omega} \right| \right), \quad (3.7)$$

where $g_1(\xi) \equiv \ln[H_1^{-1}(\xi)H_2(\xi)]$. At the singular point, $\xi = \omega$, the integral has a limit, given by $[dg_1(\xi)/d\xi]_{\xi=\omega}$. In this way, one bypasses the difficulties caused by the principal part integration. The variables $\langle n, \rangle$, $\langle n_i, \rangle$, and $\text{Im}C$ have been self-consistently determined in Sec. III for each set of values of parameters. The solution together with the evaluated functions of M_r and N_r are used here as input parameters. To simplify the calculation, we use the asymptotic expansion for the digamma function¹⁰ which appears in A_1 and A_2 . This yields

$$\text{Re}\psi\left(\frac{1}{2} \mp iy\right) = \frac{1}{2} \ln\left(\frac{1}{4} + y^2\right).$$

The evaluation of P_0 requires the handling of a two-fold integration since the integral $Q_3(\omega)$ is embedded within the outer integral for P_0 . The integrals are evaluated by a program based on Romberg integration techniques. The ranges of both the inner and outer integrations have been divided into several appropriate subranges so that each subrange can be computed smoothly and efficiently. The final result should be accurate to better than 1%.

We have computed the magnetoresistivity for arbitrary values of H and T . The results on the temperature variation of the magnetoresistivity is displayed in Fig. 6 for a number of values of the external magnetic fields. The same results are shown in Fig. 7 as a function of the external magnetic field H . The Kondo temperature has been fixed at 2 K. Figures 6 and 7 indicate general depreciation of the magnetoresistivity in the presence of the external magnetic field. The applied field tends to suppress the anomalous resistivity by "freezing out" the local magnetic moment and depreciating the spin-compensated state which is held responsible for the Kondo effect. The phenomena can be interpreted in terms of the product of two competing mechanisms. The first is due to the spin-flip scattering process which is governed by the conduction-electron scattering amplitude. As the thermal fluctuation decreases due to the lowering of temperature, the spin-flip scattering is greatly enhanced. This results in a logarithmic rise of the resistivity as the temperature decreases

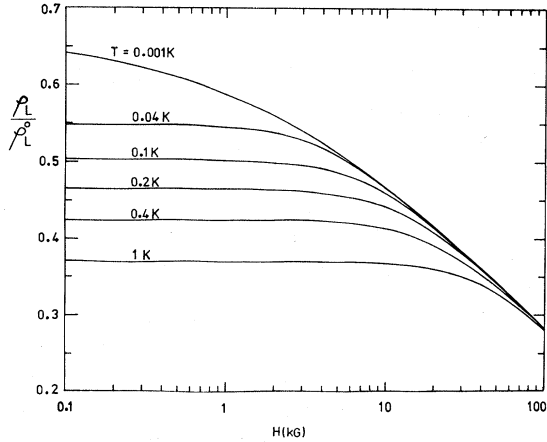


FIG. 7. Magnetoconductivity ρ_L , in reduced units, as a function of external magnetic field for a number of temperatures.

through T_K . In zero field, only this mechanism exists. In the presence of an applied field H , the spin-flip scattering process is gradually “frozen out” due to the aligning of the impurity spins by the field. When the value of H/T gets sufficiently large, the “freezing-out” mechanism becomes dominant and the spin-flip scattering process becomes inhibited. The depreciation of the magnetoconductivity is then governed by the second mechanism until all the spins are completely aligned.

The calculated family of curves of the magnetoconductivity in Fig. 6 exhibits consistent plateau regions at low temperatures. The results agree well qualitatively with the experiments of Fenton¹¹ on Fe and Cr in a Cu(Au) matrix and with those of Daybell and Steyert¹² on Cr in Cu. However, we do not obtain the resistivity peaks at low temperatures, which were observed in the measurement of Monod¹³ on Mn in Cu. The plateau behavior of the resistivity at low temperatures has not been obtained in previous calculations.^{4,7,8} The exact calculations of More and Suhl⁷ and of Bloomfield, Hecht, and Sievert⁴ produce broad peaks at low temperature.

Close scrutiny of Figs. 6 and 7 when compared with the experimental results of Fenton¹¹ indicates that discrepancies exist at low temperatures ($T \ll T_K$, $H \rightarrow 0$) and low fields ($H \ll H_K$, $T \rightarrow 0$). The T^2 and H^2 variations in these regimes are not obtained. This is apparently due to the defect of the truncation process. The truncation scheme used in this calculation is equivalent to the Nagaoka decoupling procedure¹⁴ in which the Dyson's equation for the single-electron propagator is approximated to

$$G = G_0 + G_0 t G_0 .$$

The higher-order terms that must come in at low

temperature and low field have been neglected. Corrections can be achieved either by using some ground-state *Ansatz*¹⁵ or by renormalizing one of the Green's functions in the second term.¹⁶ The studies of Lam¹⁶ are confined to zero-field case. The presence of an external field destroys the spherical symmetry of the system. The difficulties are substantially increased and new approaches are yet to be sought to include the renormalization effect in the field-dependent study.

The magnetoconductivity is related to the ψ matrix via (3.4). The structure of ψ is displayed in Fig. 8 in which the function $\text{Re}\psi'(\omega + H - i\delta)$ is plotted against ω for $T = 0.1$ K and a number of fields. The curves exhibit negative troughs which vary sensitively with fields. The trough of the zero-field curve is not situated at the Fermi level $\omega = 0$ as our system lacks particle-hole symmetry. The area under the curve when integrated gives a large negative contribution. When the field is increased, the trough moves to the left, the total negative area is reduced by the creation of a certain positive area in the $(-\text{Re}\psi, -\omega)$ region. Consequently this causes the reduction of the magnetoconductivity as the field increases.

The negative magnetoconductivity is defined as

$$-\frac{\Delta\rho_L(H, T)}{\rho_L(0, T)} = \frac{\rho_L(0, T) - \rho_L(H, T)}{\rho_L(0, T)}, \quad (3.8)$$

the field dependence of which is shown in Fig. 9 for a number of temperatures. This enables us to make a direct comparison with the respective experimental results of Berman and Kopp,¹⁷ Rohrer,¹⁸ and Read and Guenault¹⁹ on Au-Fe, Au-Mn, and Cu-Cr alloys. The agreement is qualitative but good.

As mentioned earlier, the depreciation of the

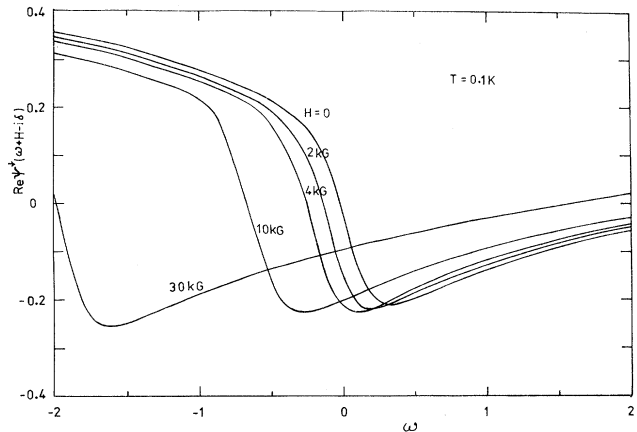


FIG. 8. Real part of the ψ matrix, $\text{Re}\psi'(\omega + H - i\delta)$, at 0.1 K as a function of the energy ω for a number of external magnetic fields; $\omega = 0$ corresponds to the Fermi energy.

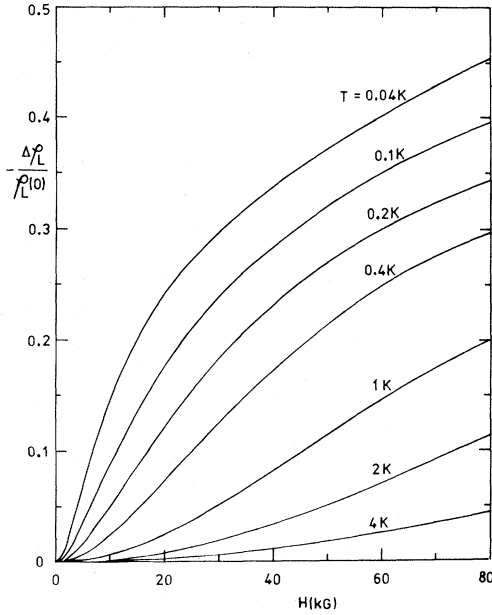


FIG. 9. Negative magnetoresistivity $-\Delta\rho_L$, in reduced units, as a function of external magnetic field for a number of temperatures.

magnetoresistivity is a result of the "freezing out" of the local magnetic moment. It is therefore interesting to see how the two quantities are related to each other. Figure 10 shows the variation of the negative magnetoresistivity with the square of the impurity magnetization for temperatures around and above T_K . Linear variations are obtained but the slopes are temperature dependent. The perturbation calculation of Béal-Monod and Weiner⁸ has shown that the negative magnetoresistivity varies with the square of the bulk magnetization for $T > T_K$. The linear variation in Fig. 10 is in agreement with their result although our M_d represents only the impurity magnetization. The strong temperature dependence of the slopes has been observed in Cu-Fe alloys (see Fig. 3 of Ref. 8 and Ref. 13).

In a preliminary report,²⁰ we have derived an approximate but analytic expression for the magnetoresistivity using Eqs. (3.2), (3.6), and (1.2)-(1.23). The result yields

$$\frac{\rho_L(H, T)}{\rho_L^0} = \frac{1}{2} \left(1 - \frac{a_1\tau + a_2}{(\tau^4 + e_1\tau^2 + e_2\tau + e_3)^{1/4}} \right), \quad (3.9)$$

where

$$\tau = \ln[(\pi^2 T^2 + H^2)^{1/2} / H_K],$$

$$a_1 = e(0) / [1 + e^2(0)]^{1/2},$$

$$a_2 = 3\pi(d' + d'') / 4[1 + e^2(0)]^{1/2},$$

$$e_1 = \left(\frac{3}{2}\pi\right)^2 [2(1 + \text{Re}C) - 2F_1(0)(d' - d'')]$$

$$+ 2F_1^2(0) + (d' - d'')^2],$$

$$e_2 = 2\left(\frac{3}{2}\pi\right)^2 [2F_1(0) - (d' - d'')] \times [\text{Im}C + e(0)(d' - d'')],$$

$$e_3 = \left(\frac{3}{2}\pi\right)^4 \{ [1 + \text{Re}C + (d' - d'')F_1(0) - F_1^2(0)]^2 + [\text{Im}C + e(0)(d' - d'')]^2 \}.$$

In obtaining the above expression, we have neglected the quantities M_0 , N_0 , $(H_1^{-1}/H_2)^{\pm 1/4}$ and the phase factor $Q_3(\omega)$ in the ψ matrices (1.3) and (1.4). The energy-averaging effect is ignored in (3.6). These approximations are examined in the exact calculation. The quantities $M_0/3\pi$ and $N_0/3\pi$ exhibit little variations as indicated in Figs. 4 and 5, and therefore can be omitted in comparison with the unity and $e(0)$ factors. The ratio $(H_1^{-1}/H_2)^{\pm 1/4}$ is of the order of unity. The contribution from the phase factor is small as far as the resistivity is concerned. Thus, to a good approximation, it can be discarded. However, it is not too good an approximation to neglect the energy averaging of the relaxation times. This causes the high-field curves to decay faster than they should be as the temperature increases across T_K . This is evident from a direct comparison between the exact result (Fig. 6) and that (Fig. 1 of Ref. 20) calculated from (3.9). Nevertheless, the qualitative behavior of the curves remain unaffected.

The simple analytic expression obtained in (3.9) gives a good description of the magnetoresistivity of dilute magnetic alloys for general values of fields and temperatures except the limiting cases: $T \ll T_K$, $H \rightarrow 0$ and $H \ll H_K$, $T \rightarrow 0$. It reduces to Theumann's²¹ and Mamada and Takano's,²² and hence Hamann's²³ equation at zero field. In the limit $T > T_K$ or $H > H_K$, it can be expanded to yield

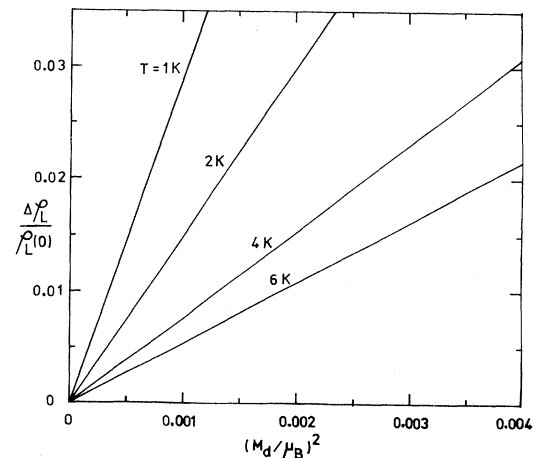


FIG. 10. Negative magnetoresistivity $-\Delta\rho_L/\rho_L(0)$, versus the square of the impurity magnetization, $(M_d/\mu_B)^2$, for a number of temperatures above and around T_K .

the perturbation results of Béal-Monod and Weiner.⁸ As an illustration, we derive the high-field expansion of (3.9). It yields

$$\frac{-\Delta\rho_L(H, T)}{\rho_L(0, T)} = 1 - \frac{e_1}{8} \left(\frac{\Delta}{\pi\epsilon_d} \right)^2 \left(1 + \frac{2\Delta}{\pi\epsilon_d} \ln \frac{H}{D} \right) \quad (H > H_K > T), \quad (3.10)$$

where for simplicity, we have neglected the small a_2 term and have approximated a_1 to unity. The negative magnetoresistivity is found to increase as a function of $\ln H$. This result was obtained theoretically by Béal-Monod and Weiner⁸ and confirmed experimentally by Berman and Kopp.¹⁷

IV. HALL EFFECT

In general, the Hall coefficient in a "two-band" model of spin-up and spin-down conduction electrons is given by²⁴

$$R = \frac{\sigma_{HT}}{\sigma_{ET}^2 + H^2 \sigma_{HT}^2}, \quad (4.1)$$

where

$$\sigma_{HT} = \sigma_{H\uparrow} + \sigma_{H\downarrow}, \quad \sigma_{ET} = \sigma_{E\uparrow} + \sigma_{E\downarrow}, \quad (4.2)$$

$$\sigma_{E\sigma} = -\frac{e^2}{3} \int_{-\infty}^{\infty} \frac{v^2(\omega) \rho(\omega) \tau_{\sigma}^2(\omega) (\partial f^{\sigma} / \partial \omega)}{1 + \omega_c^2 \tau_{\sigma}^2(\omega)} d\omega, \quad (4.3)$$

$$\sigma_{H\sigma} = -\frac{e^2 \omega_c}{3H} \int_{-\infty}^{\infty} \frac{v^2(\omega) \rho(\omega) \tau_{\sigma}^2(\omega) (\partial f^{\sigma} / \partial \omega)}{1 + \omega_c^2 \tau_{\sigma}^2(\omega)} d\omega. \quad (4.4)$$

For low and moderate fields, we can assume $\omega_c \tau_{\sigma} \ll 1$, ω_c being the cyclotron frequency and drop terms of the order $(\omega_c \tau_{\sigma})^2$. Also, we have put $v^2(\omega) = v_F^2$ and $\rho(\omega) = \rho_0$. The Hall coefficient is then simplified to give

$$R/R_0 = 2P_1/P_0^2, \quad (4.5)$$

with

$$P_1 = \int \left(\frac{-(\partial f^{\uparrow} / \partial \omega)}{[1 - \text{Re}\psi^{\uparrow}(\omega + i\delta)]^2} + \frac{-(\partial f^{\downarrow} / \partial \omega)}{[1 - \text{Re}\psi^{\downarrow}(\omega - i\delta)]^2} \right) d\omega \quad (4.6)$$

and

$$R_0 = \pm 1/N |e| c, \quad (4.7)$$

where R_0 is the zero-field Hall coefficient and P_0 is given in (3.4). We have preserved the energy averaging of τ_{σ} and τ_{σ}^2 in the above equations. As discussed in Sec. III, the energy averaging of the lifetimes may not be small and it is not too good an approximation to discard it. However, if one ignores the energy averaging effect for the sake of mathematical simplicity, the Hall coefficient will take the simple form of

$$\frac{R}{R_0} = 2 \frac{\tau_{\uparrow}^2(-H) + \tau_{\downarrow}^2(H)}{[\tau_{\uparrow}(-H) + \tau_{\downarrow}(H)]^2}. \quad (4.8)$$

This expression has been adopted in various calculations.^{8,25}

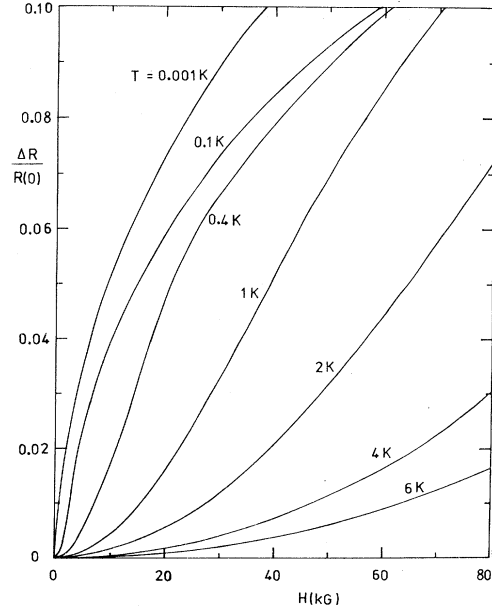


FIG. 11. Hall coefficient $\Delta R/R(0)$ as a function of external magnetic field for a number of temperatures.

The Hall coefficient has been computed for arbitrary values of H and T using the general expression (4.5) and (4.6). The computing technique has been described in Sec. III. Figure II shows the results for the Hall coefficient in the form

$$\frac{\Delta R}{R(0)} = \frac{R(H, T) - R(0, T)}{R(0, T)} \quad (4.9)$$

as a function of applied magnetic field H for a number of temperatures. These temperatures are spaced evenly around T_K which is fixed at 2 K. The Hall coefficient is found to increase generally with the magnetic field, more rapidly for temperatures below T_K . The curves give zero slopes for $H \rightarrow 0$. This can be shown easily by stretching the low-field curves using a logarithmic scale. Our results are therefore in general agreement with the calculations of More,²⁵ Béal-Monod and Weiner,⁸ and Giovannini²⁶ (Fig. 3 of Ref. 26), based on the usual s - d exchange model.

Experimental observations on the field and temperature dependence of the Hall effect have been studied by various authors^{27,28} covering the alloys Au - Fe , Cu - Cr , Cu - Fe , Cu - Mn , Au - Mn , and Ag - Mn . Owing to the complexities of the system and the difficulties²⁹ of extracting the correct spin component from the total measured effect, the actual field and temperature dependence of the spin contribution is not entirely clear. This is further complicated by the fact that there are probably two types of contributions to the spin component. The first is the "normal" contribution associated with the spin-flip scattering. The second is the anom-

alous component, the origin of which is currently thought to arise from the skew scattering of the electrons, either by individual localized moments^{26,30} or by ferromagnetic clusters of solute atoms.²⁷ The spin effect on the isothermal field dependence of the Hall coefficient (or Hall resistivity) has been analysed by Alderson and Hurd²⁷ and others.²⁸ For systems like *Cu-Mn*, *Au-Mn*, and *Ag-Mn*, the spin component can be attributed to the "normal" contribution arisen from spin-flip scattering. The Hall coefficient in this case shows a general increase with the magnetic field. This agrees qualitatively with the isothermal curves presented in Fig. 11. For other systems, the spin component is apparently dominated by the skew scattering effect. As a consequence, the Hall coefficient becomes a decreasing function of H .^{26,30}

The temperature dependence of the Hall coefficient is shown in Fig. 12 for various values of applied fields. The Hall coefficient increases with decreasing temperatures. The variation is somewhat hyperbolalike for temperatures above the Kondo temperature. For $T < T_K$, the curve tends to level off momentarily before a further increase at very low temperatures. This behavior which is more pronounced at high fields is likely a manifestation of the many-body effect at temperatures below T_K . Though the temperature dependence of the Hall effect has been measured by Hurd and Alderson,²⁷ the spin component has not been quantitatively separated out. So far as regards the

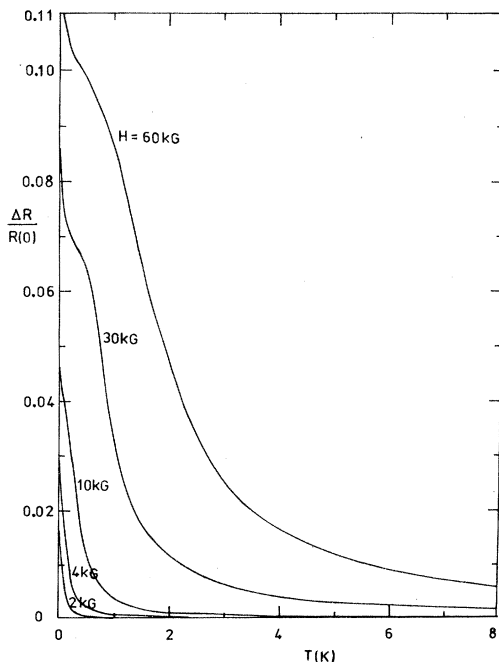


FIG. 12. Hall coefficient $\Delta R/R(0)$ as a function of temperature for a number of external magnetic fields.

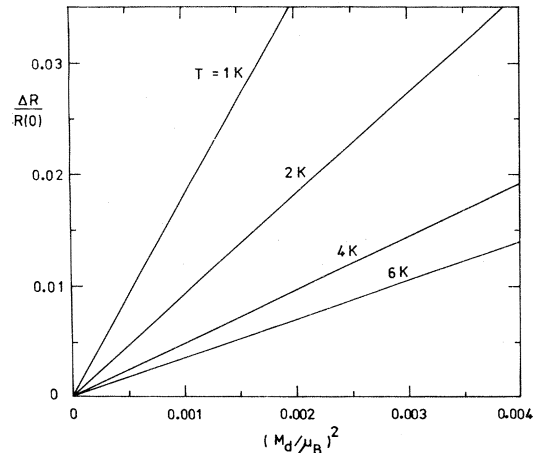


FIG. 13. Hall coefficient $\Delta R/R(0)$ versus the square of the impurity magnetization, $(M_d/\mu_B)^2$, for a number of temperatures above and around T_K .

general features, the curves in Fig. 12 indicate qualitative agreement with their results. The influence of the skew scattering on the temperature dependence of the Hall effect at fixed field is still unknown. It should be interesting to have such theoretical result for comparison.

As mentioned before, it is the effect of the freezing out of the local magnetic moment which is responsible for the observed behavior in the Hall coefficient as well as the negative magnetoresistivity. Inevitably, all these quantities are related to one another. The variation of the Hall coefficient with the square of the d magnetization is displayed in Fig. 13. Linear variations are obtained but the slopes are temperature dependent, a feature similar to that observed in Fig. 10 for the negative magnetoresistivity. The relation between the Hall coefficient and the negative magnetoresistivity is shown in Fig. 14. For temperatures above the Kondo temperature, we obtain a perfect straight line for all the fields computed. This leads us to conclude that

$$\Delta R/R(0) \propto -\Delta\rho_L/\rho_L(0) \quad (T \geq T_K). \quad (4.10)$$

However, marked deviation occurs at $T < T_K$, as is evidently shown in Fig. 14. This allows us to clarify the perturbation result of Béal-Monod and Weiner,⁸ which is valid for $T > T_K$, that the Hall coefficient and the negative magnetoresistivity are proportional to each other and to the square of the bulk magnetization.

V. CONCLUSIONS

In the light of the foregoing, the main results and conclusions are summarized as follows:

(a) The results for the impurity magnetization indicate general agreement with other calcula-

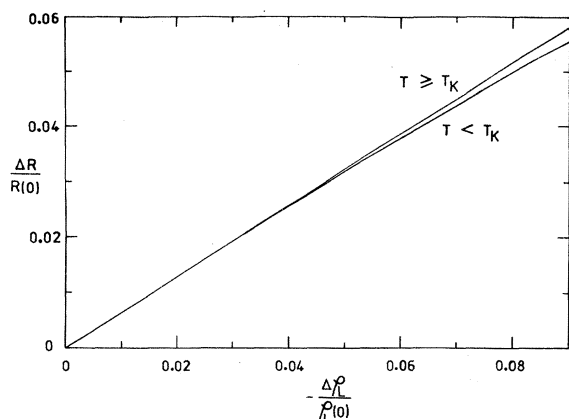


FIG. 14. Relation between the Hall coefficient $\Delta R/R(0)$ and the negative magnetoresistivity $-\Delta\rho_L/\rho_L(0)$ for temperatures $T \geq T_K$ and $T < T_K$.

tions.^{3,4} The influence of the conduction-electron polarization has yet to be worked out.

(b) The family curves of the magnetoresistivity exhibit consistent plateau regions at low temperatures. The results are in good qualitative agreement with experiments.^{11,12} However, discrepancies exist in the limiting situations: $T \ll T_K$, $H \rightarrow 0$ and $H \ll H_K$, $T \rightarrow 0$. This is due to the defect of the truncation procedure, which already showed up in

the zero-field calculations.^{21,22}

(c) An approximate but analytic expression for the magnetoresistivity is obtained, valid for general values of magnetic fields and temperatures. When expanded, it yields the perturbation results of Béal-Monod and Weiner.⁸

(d) The Hall coefficient is found to increase with fields and has a zero slope for $H \rightarrow 0$. In addition, it decreases rapidly with temperature in a hyperbolalike manner. The results for the magnetic field effects are in agreement with calculations^{8,25,26} based on s - d exchange model. They also agree with experiments^{27,28} as far as the general qualitative features are concerned. The quantitative features are, however, complicated by the presence of the anomalous contribution due to the skew scattering effect.^{26,30}

(e) For $T \geq T_K$, we find that the Hall coefficient and the negative magnetoresistivity are proportional to each other and to the square of the impurity magnetization. Marked deviations are detected at temperatures below the Kondo temperature.

ACKNOWLEDGMENTS

The author would like to thank Professor P. Peach, K. Y. Choong, H. S. Tan, Y. C. Khong, and L. C. Ching for various technical assistances in the computations and in the preparation of the graphs.

¹G. S. Poo, preceding paper, Phys. Rev. B **11**, 4606 (1975).

²See, for example, Conte de Boor, *Elementary Numerical Analysis* (McGraw-Hill Kogakusha, Japan, 1972).

³S. B. Nam and W. F. Woo, Phys. Rev. Lett. **19**, 649 (1967).

⁴P. E. Bloomfield, R. Hecht, and P. R. Sievert, Phys. Rev. B **2**, 3714 (1970).

⁵J. L. Tholence and R. Tournier, Phys. Rev. Lett. **25**, 867 (1970).

⁶J. M. Franz and D. J. Sellmyer, Phys. Rev. B **8**, 2083 (1973).

⁷R. More and H. Suhl, Phys. Rev. Lett. **20**, 500 (1968).

⁸M. T. Béal-Monod and R. A. Weiner, Phys. Rev. **170**, 552 (1968); B **3**, 145 (1971); **3**, 3056 (1971).

⁹H. Suhl, J. Appl. Phys. **39**, 1294 (1968).

¹⁰P. E. Bloomfield and D. R. Hamann, Phys. Rev. **164**, 856 (1967).

¹¹E. W. Fenton, Phys. Rev. B **7**, 3144 (1973); **5**, 3788 (1972).

¹²M. D. Daybell and W. A. Steyert, Phys. Rev. Lett. **20**, 195 (1968).

¹³P. Monod, Phys. Rev. Lett. **19**, 1113 (1967).

¹⁴Y. Nagaoka, Phys. Rev. **138**, A 1112 (1965); Prog. Theo. Phys. **37**, 13 (1966).

¹⁵Y. Kurata, Prog. Theo. Phys. **43**, 621 (1970).

¹⁶J. Lam, J. Phys. F **3**, 1197 (1973); **3**, 1207 (1973).

¹⁷R. Berman and J. Kopp, J. Phys. F **3**, 847 (1973).

¹⁸H. Rohrer, Phys. Rev. **174**, 583 (1968).

¹⁹M. Read and A. M. Guenault, J. Phys. F **4**, 94 (1974).

²⁰G. S. Poo, J. Phys. F **4**, L121 (1974).

²¹A. Theumann, Phys. Rev. **178**, 978 (1969).

²²H. Mamada and F. Takano, Prog. Theo. Phys. **43**, 1458 (1970).

²³D. R. Hamann, Phys. Rev. **158**, 570 (1967).

²⁴See, for example, J. M. Ziman, *Electrons and Phonons* (Oxford U. P., London, England, 1960).

²⁵R. M. More, Solid State Commun. **7**, 237 (1969).

²⁶B. Giovannini, J. Low Temp. Phys. **11**, 489 (1973).

²⁷J. E. A. Alderson and C. M. Hurd, J. Phys. Chem. Solids **32**, 2075 (1971); Phys. Rev. B **7**, 1226 (1973); **7**, 1233 (1973).

²⁸P. Monod and A. Friederich, in *Proceedings of the Twelfth International Conference on Low Temperature Physics, Kyoto, 1970*, edited by E. Kanda (Keigaku Publishing Co; Tokyo, 1971), p. 755; also the reference cited by A. Fert and O. Jaoul (Ref. 30).

²⁹See the discussion by J. E. A. Alderson and C. M. Hurd [Phys. Rev. B **7**, 1233 (1973)].

³⁰A. Fert and O. Jaoul, Phys. Rev. Lett. **28**, 303 (1972).